Journal of Radioanalytical and Nuclear Chemistry (2023) 332:1775–1786
https://doi.org/10.1007/s10967-023-08869-6

Diglycolamic acid coated cation exchange adsorbent for uranium removal by extraction chromatography

B. Robert Selvan[1] · A. S. Suneesh[1] · N. Ramanathan[1,2]

Received: 9 January 2023 / Accepted: 14 March 2023 / Published online: 30 March 2023

Abstract
This paper highlights the development of an extraction chromatography-based recovery of uranium using a diglycolamic acid-coated polymeric resin from low-concentration uranium- bearing solutions. Factors controlling uranium separation have been examined as a function of the pH of the aqueous medium, interfering ions, uranium concentration in the aqueous phase, duration of contact of the resin with the aqueous phase, etc. The adsorption kinetics and isotherm models are modeled with the pseudo-first and the pseudo-second-order adsorption kinetics. The outcome of the batch and column-based adsorption studies corroborates the prospect of using diglycolamic acid-coated polymeric resin to separate uranium from low-concentration feeds.

Keywords Uranium · Adsorption · Polymeric resin · Solvent impregnation · Ion exchange

Introduction

The solid phase adsorbents have captivated applications for heavy metal separation, perceptive to the toxic heavy metal removal [1, 2], metallurgy, and analytical preconcentration, to mention a few. Polymeric resins have been an ideal choice for metal ion removal among different solid-phase adsorbents developed [3–6]. Until four to six decades back, the metallurgical separations solely relied on liquid–liquid extraction techniques and the resin-based solid-phase extractions. However, the need for chelating-type metal ion-selective solid-phase adsorbents (resins) restricted the scope of solid-phase adsorbents to limited applications. Conversely, the pioneering works of Warshawsky, Grinstead, Kroebel, and Mayer have led to the development of Solvent Impregnated Resins (SIRs) in which suitable metal ion selective chelating ligand anchored in a neutral polymeric resin was used for separation. The advent of SIRs [7–10] reduced the cost of chelating resins and capacitated incorporating a variety of chelating-type ligands on various resins.

The increasing requirement for uranium [11, 12], a naturally occurring radioactive element used as fuel in thermal nuclear reactors for producing electricity by harnessing the energy produced by nuclear fission reaction, is primarily sourced from uranium minerals present in the earth's crust. It is a matter of great concern as it is declining faster because of its enhanced utilization. Seawater is recognized as a future source of uranium. Uranium recovery from seawater is one of the active areas of research. However, the natural abundance of uranium in seawater is approximately 3 $ngmL^{-1}$ [13]. Assuming that most of the area on earth is covered by the sea, the amount of uranium in seawater is several times higher than its sources in the earth's crust. The health hazard of uranium because of its chemical and radiotoxic nature [14–17] is another severe issue despite its beneficial use. Uranium's presence in drinking water sources has also increased due to various human activities involving uranium recovery from mineral sources [18–20]. Therefore, by considering the health hazards caused by uranium [21], according to World Health Organization (WHO) guidelines, the allowed limits of uranium in drinking water should be less than 30 $ngmL^{-1}$ [22]. In view of the above, the uranium separation method from the lean sources of uranium, wherein uranium concentration levels are appreciably low,

✉ A. S. Suneesh
suneesh@igcar.gov.in

✉ N. Ramanathan
nram@igcar.gov.in

[1] Materials Chemistry and Metal Fuel Cycle Group, Indira Gandhi Centre for Atomic Research, Kalpakkam 603102, Tamil Nadu, India

[2] Homi Bhabha National Institute, Indira Gandhi Centre for Atomic Research, Kalpakkam 603102, Tamil Nadu, India

is challenging. The usual Ammonium Di-Uranate (ADU) precipitation method is unsuitable for uranium separation from the above feeds as the uranium concentration levels are appreciably low. Because of the superior separation capability and selectivity, a variety of solid-phase adsorbents have been studied for uranium separation from different low-level uranium sources such as seawater and uranium-contaminated mine water sources, and so on [23–27].

Amidoxime is one of the popular reagents extensively studied for uranium separation from ultra-low uranium feeds [28]. Various amidoxime-based materials have been developed for uranium separation by different research groups. The preferential selectivity of amidoxime moiety is considered responsible for the superior separation of uranium. Numerous research works in the literature dealt with preparation, adsorption, and mechanistic aspects of uranium separation by amidoxime groups [29–31]. Researchers have also developed several other adsorbents, which are either cation exchangers or are the ones with amine functionality [32–36]. The chemical stability and multi-step synthetic procedures for the amidoxime-based reagents or amine-based reagents have restricted them to academic interest only. The advantage of cation exchangers, on the other hand, rests on their recyclability. In the present context, we developed a diglycolamic acid-coated resin to separate uranium from the ultra-low-level uranium-bearing feed solution. The diglycolamic acid-coated resin is cost-effective as the diglycolamic acid is easy to prepare.

Diglycolamic acid is a typical cation exchanger, expected to form a cation exchange type complex with metal ions in a low acidic medium. Other researchers and we have previously studied diglycolamic acid-type ligands [37, 38]. We studied the mutual separation of trivalent lanthanides and actinides using diglycolamic acid-based adsorbents [37]. Likewise, Ilaiyaraja and coworkers investigated the sorption features of uranium from uranium-contaminated aqueous solutions [38]. The large-scale separation feasibility of the uranium from sub-micron level feed solution has yet to be studied. In contrast to the elsewhere reported studies on diglycolamic acid-based adsorbents, the present work's interest is to remove uranium from sub-micron level feed solutions. Moreover, these studies are essential because of the increased focus on developing adsorbents for uranium recovery from sea water. The complicated aqueous chemistry of uranium in sea water and the problematic separation chemistry owing to several interfering metal ions such as vanadium are significant challenges of uranium recovery from such feeds. This paper will also discuss the effectiveness of the solvent impregnation technique in developing a solid phase adsorption technique. To establish the separation effectiveness, the diglycolamic acid coated resin was studied for uranium separation from aqueous solutions under different pH conditions and various concentrations of uranium. The kinetics of uranium removal was also investigated. The recycling capability of the adsorbent has also been studied. The limited data sources restricted to the laboratory sorption experiments on uranium sorption by diglycolamic acid-based sorbents also call for developing a large-scale separation attempt to augment the diglycolamic acid based solid phase adsorbents. In view of this, a demonstration experiment based on column chromatography was also performed to understand the bench-top scale separation efficiency of the system.

Experimental methods

Materials and methods

The uranium selective ligand, diethylhexyldiglycolamic acid (HDEHDGA), was prepared by reacting diglycolic anhydride and bis-2-ethylhexylamine. Synthesis and characterization of HDEHDGA have been dealt with in many works of literature [38–41]. Briefly, diglycolic anhydride (10 g, 50 mmol) and bis-2-ethylhexylamine (10 g, 50 mmol) were reacted at 60 °C in the presence of chloroform solvent for 12 h. After 12 h, the crude reaction product was separated and washed several times with 1 M HCl (10 mL × 5 times), followed by millipore water (10 mL × 10 times). HDEDGA was separated from the solvent phase by distillation in a rotary evaporator. The structure of HDEHDGA is shown in Fig. 1. The diglycolic anhydride (Aldrich, 99%) and bis-2-ethylhexylamine (99%) were used without any purification. All other chemicals used for the experiment, such as chloroform (RANKEM, AR), nitric acid (RANKEM, AR), acetic acid (RANKEM, HPLC), sodium acetate (ALDRICH, 99%), Tulsion ADS 400 was procured from M/s Thermax, India. Tulsion ADS 400 is a polyacrylic polymer of particle size 0.3–1 mm, (18–50 mesh), a surface area of 375 m^2 /g. The resin was washed with water, followed by acetone several times, and dried in air for 48 h before its use. The dried resin was used for coating. Different concentrations of coated resin were prepared by varying the amount of diglycolamic acid ligand. The dried resin was dispersed in ethanol, where diglycolamic acid was initially dissolved. The solution was agitated in a shaker for 10 h. The solvent was removed after 10 h by filtration, and the resin was dried in air for 48 h. The weight difference analysis of resin before and after coating showed that the loss of diglycolamic acid was less than 0.5%.

The optical absorbance of uranium samples was determined by a Fiber optic coupled (Avantes, UK) UV–Visible spectrophotometer. An Arsenazo complex of uranium was prepared for this purpose. Suitable aliquots of uranium samples were added to a mixture of Arsenazo III, sulfamic acid, and nitric acid in a 10 mL standard flask. The

Fig. 1 Structure of HDEHDGA

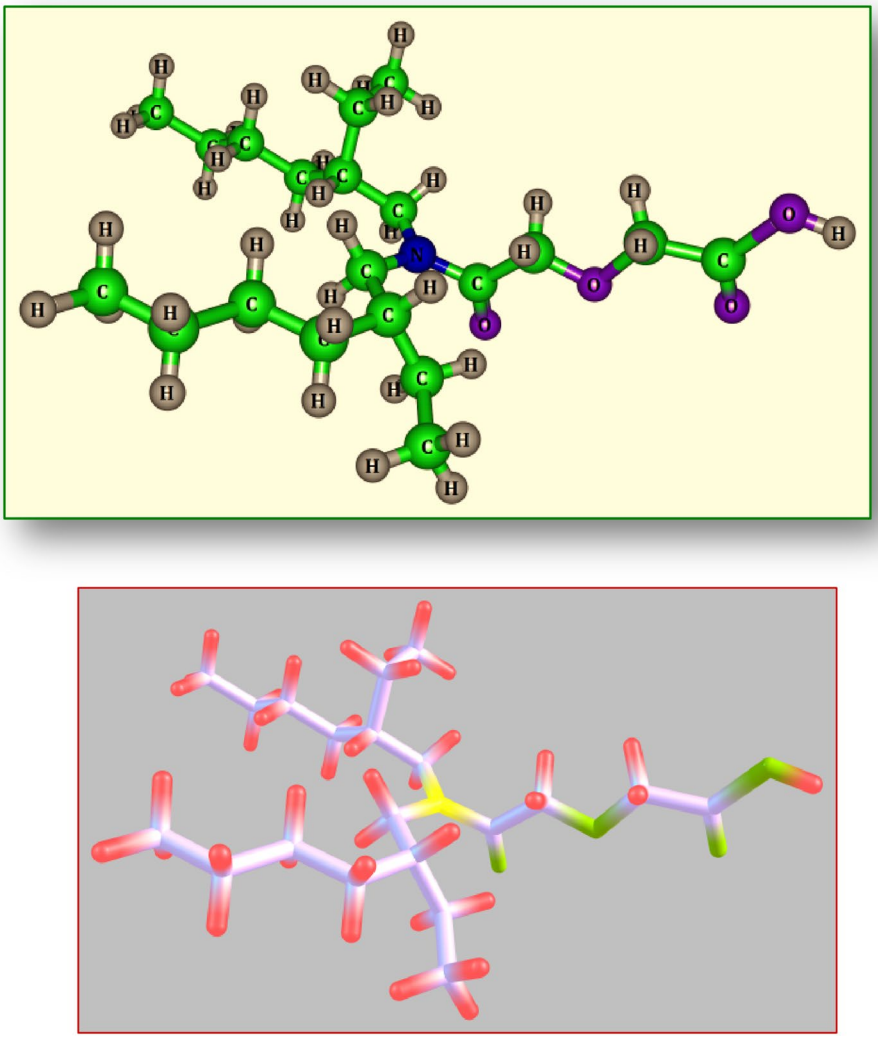

absorbance of the uranium-Arsenazo complex was measured at a wavelength of 560 nm after 3 h. The concentrations of the different uranium samples were calculated from the calibration plot generated by measuring the absorbance of standard uranium samples from 1 to 10 µg mL^{-1} (supplemental Fig. S1).

Adsorption studies

The uranium-adsorption trend to the resin was examined by monitoring the concentrations of uranium present in the aqueous phase before and after the contact with the resin. 10 mL of uranium-containing solutions, prepared in which uranium concentration was varied from 10 to 1000 µg mL^{-1}in different experiments, were equilibrated with 50 mg of the resin for 7 h. The resin dispersed in the solution present in a closed glass vial was agitated in a shaker with a speed of 250 rpm. All equilibration experiments were performed at 298 K. The concentration of uranium, before and after the contact with the resin, was measured by UV–Visible spectrometer, as discussed in "Materials and methods" section. Aqueous solutions at different pH values were prepared by mixing suitable concentrations of acetic acid and sodium acetate. The adsorption efficiency was expressed in terms of distribution coefficient (described in Eq. 1) or as the amount of uranium loaded per gram of resin. The error involved in these experiments could be within ± 1%. In order to understand the repeatability of the values, all similar equilibration studies were measured for four different samples with the same conditions.

The distribution coefficient (K_d) of uranium adsorbed to the resin was calculated from Eq. 1.

$$K_d = \frac{[U]_{Ori} - [U]_{af}}{[U]_{af}} \frac{Volume\ of\ aqueous\ solution}{Weight\ of\ adsorbent} \left(mL.g^{-1}\right) \quad (1)$$

where $[U]_{ori}$ and $[U]_{af}$ refersto the concentrations of U (VI) present in the aqueous solution before and after the contact of the resin with the aqueous phase.

For the measurement of the optimum duration required for effective adsorption of uranium in the resin, the kinetic experiment was also performed with uranium (100 µg mL^{-1} of uranium in 10 mL acetate buffer at pH 6) bearing acetate buffer solutions containing 50 mg of dispersed resin beads. For this purpose, seven different glass vials containing uranium and resin each were equilibrated for different time durations such as 10, 30, 60, 120, 240, 360, 420 min. The uranium concentrations from the different time duration collected from different solutions were measured by the method discussed above.

The adsorption isotherm experiments were also performed by equilibrating 10 mL of uranium present in acetate buffer, adjusted to pH 6 with 50 mg of the resin, for seven hours. For this experiment, seven different vials were taken, each containing uranium at different concentrations varied from 10 to 1000 µg mL^{-1}. The amount of uranium adsorbed to the resin was measured as discussed above.

Elution of uranium from the resin

The elution behavior of uranium loaded to the resin was studied by using 0.1 M and 0.5 M nitric acid. Elution studies were also performed by batch experiments that involved contacting uranium-loaded resins with fresh solutions of nitric acid (0.1 M or 0.5 M). For the adsorption of uranium to resin, 10 mL solutions of 100 µg $mL^{-1}$of uranium present in the aqueous phase were equilibrated with 50 mg of the resin. The uranium adsorbed resin phase was separated from the aqueous phase after ensuring the quantitative adsorption of uranium and was further contacted with elution solution (10 mL of 0.1 M or 0.5 M nitric acid). Uranium present in the aqueous phase after the contact of the uranium-loaded resin with nitric acid was analyzed by UV Visible spectrometry.

Column adsorption of uranium

Adsorption of uranium to HDEHGA resin under dynamic mode was studied by passing 150 mL of uranium (200 µg mL^{-1}) bearing acetate buffer feed solution to a glass column having 8 mm diameter at a flow rate of 0.2 mL/min. 10 mL fractions of the effluent samples were collected and were analyzed for uranium by spectrophotometry.

Stability of the resin and reusability

The stability of the resin in an aqueous environment was studied. This experiment involves the treatment of the resin with an aqueous phase (pH 6, carbonate medium having 0.05 M carbonate). 1 g of the resin was soaked in 25 mL aqueous phase in a round bottom flask, and the solution was subjected to stirring with the help of a magnetic stirring unit. 50 mg of resin was drawn once in three days and equilibrated with 10 mL (pH 6), an aqueous solution containing 100 ppm uranium. The uranium adsorption efficiency of the resin was tested by measuring the amount of uranium extracted from the resin phase. A similar exercise was carried out for thirty days.

The reusability of the resin for multiple cycles of operation has been studied. A typical experiment involves measuring the adsorption efficiency of uranium for HDEHDGA-coated resin. 50 mg of resin was contacted with 10 mL aqueous solution (0.05 M carbonate at pH 6). The adsorbed uranium was recovered from the resin phase by 0.5 M nitric acid. Another adsorption study was further carried out using recycled resin. Uranium loaded to the resin was again recovered using 0.5 M nitric acid. The uranium adsorption and recovery were monitored by measuring the uranium concentration in the aqueous phase. This exercise was repeated for five cycles of operation.

Results and discussions

Impregnation of HDEHDGA to polystyrene resin

Solvent impregnation is a traditional approach for incorporating ligands into various resins and employing them for adsorption. It has been known from multiple works of literature, significantly by Warsharsky and several others, that SIR leads to the physical entrapment of ligands to the resin structure. It is, therefore, tough to characterize solvent impregnation. Weight analysis of un-impregnated and impregnated resin is a standard technique to assay the amount of ligand impregnated to the resin. The weight gain analysis observed solvent impregnation of HDEHDGA to the polystyrene resin before and after the impregnation. Assuming there is no loss of HDEHDGA during the solvent filtration from the resin phase, 40% loading of HDEHDGA was observed from the weight gain analysis. Analysis of ethanol separated from the impregnation medium was analyzed by FTIR, and the spectrum did not show the presence of HDEHGA, indicating that the HDEHDGA would have been quantitatively adsorbed to the resin matrix. Since solvent impregnation relies on the physical adsorption of HDEHDGA, the chemical structure of HDEHDGA is expected to be retained the same after the impregnation. Figure 2 shows the FT-IR spectrum of 40% HDEHDGA impregnated with polystyrene resin, which indicated the signatures of hydroxyl, carbonyl, and etheric groups that could be present in HDEHDGA, as reported earlier [38].

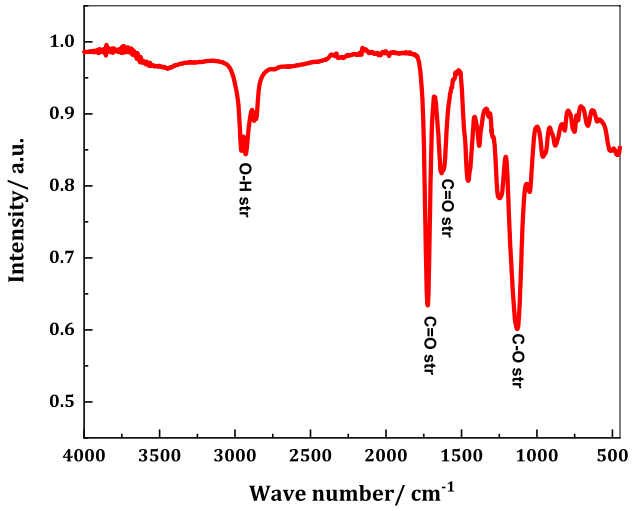

Fig. 2 FT-IR spectrum of HDEHDGA-coated polystyrene resin

Adsorption behavior of uranium by HDEHDGA-coated resin

Uranium adsorbed to the coated resin (containing 40% HDEHDGA) increased from pH 1 to pH 6, followed by a slight decrease after pH 7, as shown in Fig. 3. Figure 3 shows the variation of distribution coefficients of uranium as a function of aqueous solutions pH. Since the aqueous solution is an acetate buffer, uranium is expected to be in acetate form either as $UO_2(CH_3COO)_2$ or $[UO_2CH_3COO]^+$. The HDEHDGA is a cation exchanger with a pKa value of approximately 5; therefore, the conjugate base, $DEHDGA^-$ is supposed to be stable above pH 5. The excessive adsorption of uranium at pH 6 is attributed to the stability of $DEHDGA^-$ above pH 6. Above pH 7, due to the hydrolysis

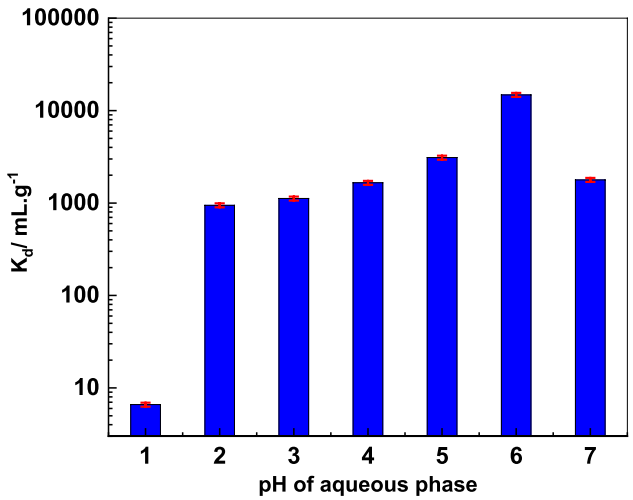

Fig. 3 Adsorption behavior of U(VI) to HDEHDGA resin as a function of pH

of uranium, other species of uranium, such as $UO_2(OH)_2$, compete with $UO_2(CH_3COO)_2$ and $[UO_2CH_3COO]^+$. The decrease in adsorption of uranium above pH 7, therefore could be due to the competition between $UO_2(CH_3COO)_2$ /$[UO_2CH_3COO]^+$and the hydrolyzed species of uranium ($UO_2(OH)_2$). The cation exchange reaction between HDEHDGA and $UO_2(CH_3COO)_2$ (expressed as M^{2+} for simplicity) can be illustrated as follows.

$$2H^+DEHDGA^- + M^{2+} \Leftrightarrow M(DEHDGA)_2 + 2H^+ \quad (2)$$

The increase in distribution coefficient from pH 1 to 6 could be attributed to the formation of M(DEHDGA) as the predominant species of uranium in this pH range is $UO_2(CH_3COO)_2$.

Kinetics of adsorption of uranium on HDEHDGA coated resin

Figure 4 shows the amount of uranium adsorbed to the coated resin at different durations of contact between resin and uranium solutions (50 mg uranium in acetate buffer at pH 6, 298 K). The amount of uranium adsorbed to the resin was 10 mg g^{-1} in just 10 min and was increased to 68 mg g^{-1} at 360 min, and consequently, the value stays constant forever. This indicates that within 360 min, equilibrium is established between uranium and HDEHDGA (present in the resin phase). Therefore, all the adsorption studies were performed for 420 min to ensure quantitative adsorption of uranium to the resin. Furthermore, the data

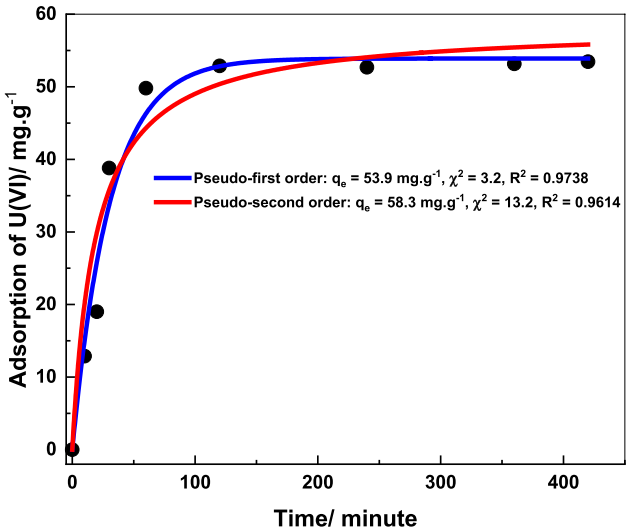

Fig. 4 Kinetics of adsorption: U(VI) adsorbed as a function of time, modeled with PFO and PSO. Adsorbent: 50 mg of HDEHDGA resin, Aq. Phase: Acetate buffer at pH 6 containing 100 µg mL^{-1} of uranium (10 mL.)

on the kinetics of uranium adsorption (shown in Fig. 4) was modeled with a few of the well-established kinetic models for metal ion adsorption on the resin surface. It has been generally presumed that the kinetics of metal ion adsorption on the resin surface is influenced by the chemical reaction between the metal ion and the target site in the resin (ligand in this case) and the role of diffusion of metal ions to the resin surface. This could be because diglycolamic acid is a cation exchanger; the adsorption could be primarily driven by the chemical exchange of uranium with the hydrogen from the carboxylic acid group of diglycolamic acid. Of course, there can be the influence of other factors as well. Therefore, it would be too early to claim that the adsorption is directed by physisorption or chemisorption. Similar to adsorbents based on a cation exchange mechanism, the predominant adsorption mode for the diglycolamic acid system also is believed to be due to the chemical exchange. In this context, the kinetic data was modeled with the Lagergren pseudo-first-order (PFO) kinetic model, pseudo-second-order model (PSO), Film-diffusion (FD) model, and intra-particle (IPD) diffusion model. Several pieces of literature have described the theoretical background behind these models [42–45]. In short, according to the PFO and PSO models, the chemical reactions between the adsorption site and the target metal ions play a crucial role in the kinetics of adsorption and in the film-diffusion and intra-particle diffusion models, the rate of diffusion of metal ion guides the kinetics of adsorption. All these models were fitted by non-linear analysis and the closeness of fit was interpreted in terms of the non-linear regression fitting parameters (such as χ^2 and R^2).

PFO and PSO models are described by Eqs. 3 and 4

$$q = q_e\left(1 - e^{-k_1 t}\right) \tag{3}$$

$$q = \frac{q_e^2 k_2 t}{\left(1 + q_e^2 k_2 t\right)} \tag{4}$$

where q is the amount of uranium adsorbed at different durations of contact between resin and uranium, q_e is the amount of uranium adsorbed after attaining equilibrium. k_1 and k_2 are the rate constants for PFO and PSO.

The model fitting data shown in Fig. 4 describes the closeness of the experimental kinetic data with PFO, which interprets a direct single-order relation between the rate of adsorption and the number of sites available for adsorption. The closeness of PFO model can be explained in terms of the non-linear fitting parameters such as R^2 and χ^2, shown in Fig. 4, as well. Uranium adsorbed (mg g^{-1}) to the resin after attaining equilibrium, derived from the PFO model, is 53.9 mg g^{-1}.

To push it further, the role of diffusion-influenced kinetics of adsorption is modeled for the present system. IPD and FDmodels are described by Eqs. 5 and 6.

$$q = k_{id}\sqrt{t} + C \tag{5}$$

$$\ln(1 - F) = -k_{fd} t \tag{6}$$

where, K_{id} is the intra-particle diffusion rate constant. To satisfy the IPD model, the plot of q as a function of $t^{0.5}$ should result in a straight line with a slope k_{id} and intercept C. To fit into the FD model, a linear regression of the plot of $-\ln(1-F)$ versus t should result in a straight line passing through the origin.F is the fractional attainment of equilibrium ($F = q/q_e$), k_{fd} is the adsorption rate constant for FD. The results are depicted in Fig. 5, which describes the role of film diffusion (FD) for 120 min(see the fitting parameters as shown in Fig. 5). According to the film diffusion theory of adsorption, suggested by Boyd et al. and several other researchers [46–49], the microscopic film of the target metal ion formed near the adsorption site deciding the kinetics of adsorption and the overall kinetics is governed by the chemical interaction between the adsorption site and the metal ions. Conversely, the intra-particle diffusion model [50, 51] suggests the role of intra-particle diffusion of the target metal ions, along with the pores of the adsorbent, to the kinetics of adsorption. Figure 5 also depicts the modeling of the kinetics of adsorption with IPD up to 100 min. It can be seen between Figs. 4 and 5 and from the fitting parameter, R^2, that none of the models are adequately qualified to demonstrate the kinetic phenomenon fully. However, the R^2 value of above 0.95 for each of the kinetic models (PFO, PSO, IPD, FD), suggests that the adsorption kinetics

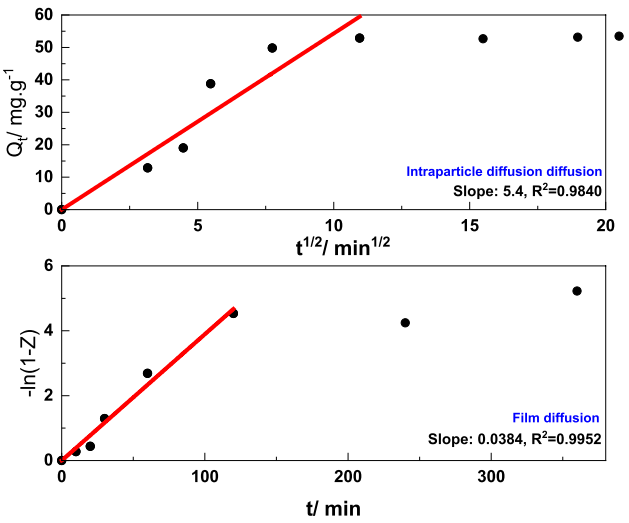

Fig. 5 Kinetics of adsorption: U(VI) adsorbed as a function of time, modeled with Intraparticle and Film diffusion models

is influenced by the role of different factors. Therefore, the kinetics of adsorption, therefore, could be explained in terms of the combined role of diffusion (i) of the metal ions towards the ligand surface(ii) diffusion of the metal ions across the microscopic film formed near to the ligand moiety, and (iii) the chemical reaction between the adsorption site and the target metal ions.

Adsorption isotherm experiments

Efficiency of the uranium adsorption by the resin at different concentrations of uranium has been studied by adsorption isotherm experimentsdepicted in Fig. 6. Uranium adsorption seems increased with increase of uranium concentration in the aqueous phase. The amount of uranium (mg g^{-1}) adsorbed to the resin, at different initial concentrations of uranium (10 µg $mL^{-1}$to 1000 µg mL^{-1}), measured from the equilibration studies was modeled to different adsorption isotherms such as Langmuir adsorption isotherm, Fruendlich isotherm, Dubinin–Radushkevich (D-R) isotherm and Tempkin isotherm (Fig. 6). Equations representing the Langmuir adsorption isotherm, Fruendlich isotherm, D-R isotherm, Tempkin isotherm models are shown in Eqs. 7, 8, 9 and 10 respectively.

$$q = \frac{q_e C_U K_L}{1 + C_U K_L} \tag{7}$$

$$q = K_F C_U^{\beta} \tag{8}$$

$$q = q_e \exp\left[-K_{ad}\left(RT \ln\left(1 + \frac{1}{C_U}\right)\right)^2\right] \tag{9}$$

$$q = \frac{RT}{b} \ln\left(A_T C_U\right) \tag{10}$$

K_F and K_L represent the Freundlich and Langmuir constants, C_U represents the uranium present in the aqueous phase (µg mL^{-1}), and β is the heterogeneity of the surface. K_{ad} represents the Dubinin–Radushkevich isotherm constant (mol^2/kJ^2). R and T are the gas constant (8.314 J/mol/K) and absolute temperature (K). $A_T$is the Temkin isotherm equilibrium binding constant (L/g) and b is the Temkin isotherm constant (Table 1).

The fitting pattern of the different adsorption isotherms with the experimental data, showed an explicit agreement with the Langmuir adsorption model (as shown in Eq. 7) that considers adsorption onto uniformly distributed adsorption sites across the resin surface. However, the heterogeneous Freundlich, Tempkin and D-R isothermadsorption models did not concur to the experimentally obtained adsorption data. This is obvious from the fitting parameters (R^2 and χ^2) derived by the non-linear regression analysis that suggests thecloseness of the experimental data with the Langmuir adsorption isotherm. It is also apparent that the Langmuir adsorption capacity (68.2 mg g^{-1}) derived from the Langmuir adsorption equation is reasonably close to the value derived by the PSO kinetic model. The adsorption capacity values of uranium derived by different adsorbents reported previously is compared in Table 2. It can be seen that the adsorption capacity exhibited by the HDEHDGAcoated resin (Tulsion ADS 400) is on par with the similar adsorbents reported elsewhere [52–59].

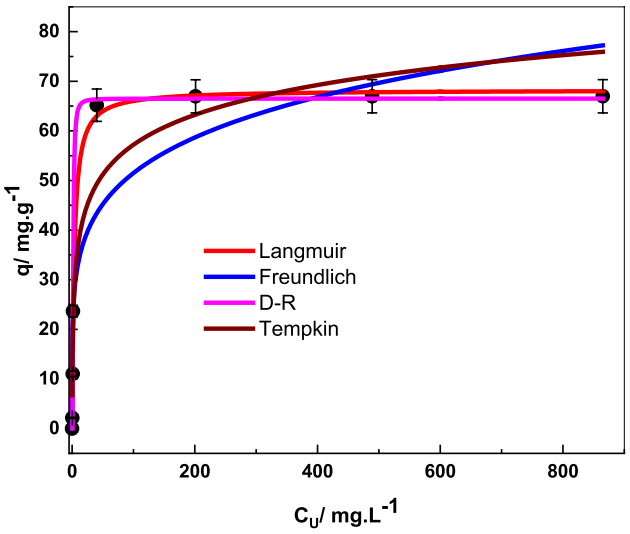

Fig. 6 Adsorption isotherm study: U(VI) adsorbed as a function of uranium concentration. Adsorbent: 50 mg of HDEHDGA resin, Aq. Phase: 10 mL of acetate buffer at pH 6 containing uranium concentration that was varied from 10 to 1000 µg mL^{-1}

Table 1 Fitting parameters of Langmuir, Freundlich, D-R and Tempkin adsorption modeled data on the adsorption of U(VI) at from different concentrations of U(VI) in the aqueous phase

Langmuir		Freundlich		Tempkin		D-R isotherm	
b	68.2	β	0.18	A_T (L/m g)	285.6	q_s(mg g^{-1})	66.2
K_L	0.28	K_F	21.6	b	7.3	K_{ad} (mol^2/kJ^2)	0.0022
χ^2	6.3	χ^2	164.6	χ^2	70.3	χ^2	9.8
R^2	0.9933	R^2	0.8337	R^2	0.9236	R^2	0.9781

Table 2 Uranium adsorption capacity of HDEHDGA compared with the adsorbents reported previously

Adsorbent	Adsorption capacity ($mg.g^{-1}$)	Aqueous medium	References
Present adsorbent	68.2	pH 6	Present study
Polyacrylamide-based chelating sorbents	65.3	pH 4	[52]
Modified mesoporous silica (MCM-41) using 5-nitro-2-furaldehyde (fural)	47	pH 5.5	[53]
Sodium Bentonite Activated Clay	11.8	pH 4.2	[54]
Clay cured with ethyl acetate (Treated clay)	37.2	pH 4.5	[55]
Thermally and chemically modified bentonite	29.5	pH 6	[56]
Amberlite XAD-4 functionalized with succinic acid	12.3	pH 4.5	[57]
Catechol functionalized aminopropyl silica gel	15.94	pH 5	[58]
Salicylaldehyde-modified mesoporous silica (Sal-APS-MCM-41)	10	pH 5	[59]

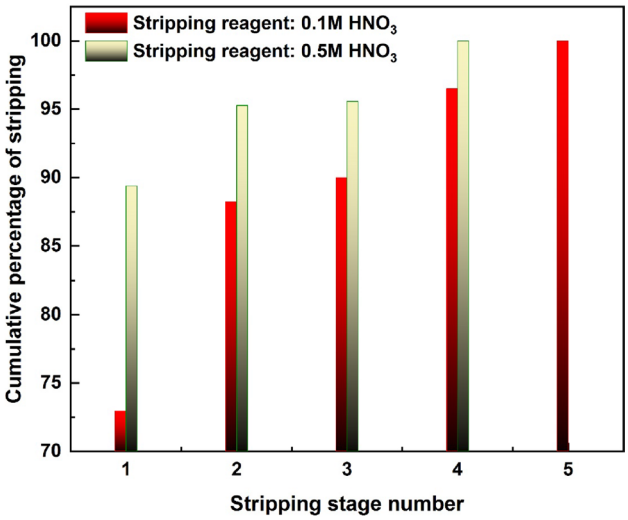

Fig. 7 Elution behavior of U(VI) from the resin phase. Adsorbent: 50 mg of HDEHDGA resin preloaded with 100 µg $mL^{-1}$of uranium. Eluting solution:10 mL of Nitric acid (0.1 or 0.5 M)

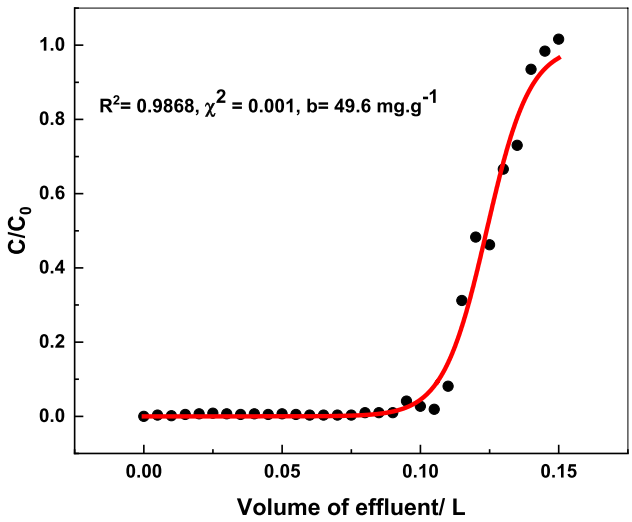

Fig. 8 Breakthrough profile of uranium adsorption onto HDEHGA resin, modeled with Thomas model. Resin phase: 0.5 g of HDEHGA resin, Feed solution: 200 µg $mL^{-1}$of uranium present in acetate buffer at pH 6. Flow-rate: 0.2 mL/min. Inner diameter of the column: 8 mm

Elution behavior of uranium from the adsorbent

Uranium exchanged to the HDEHDGA resin was eluted by nitric acid. Two different nitric acid solutions, 0.1 M and 0.5 M, were attempted for studying the elution behavior of uranium exchanged to HDEHDGA resin. Figure 7 shows the elution trend of uranium from uranium adsorbed HDEHDGA resin. The quantitative elution of uranium was accomplished in four stages with 0.5 M nitric acid on uranium adsorbed HDEHDG resin, whereas 0.1 M required a minimum of five stages.

Uranium exchange behavior in HDEHDGA resin under column mode

Uranium exchange feasibility of HDEHDGA resin under a dynamic mode of operation was investigated by column chromatography under fixed bed conditions. The amount of uranium adsorbed to the packed resin was analyzed as a function of the fraction of uranium present in effluent samples (C) with reference to its concentration levels in the feed solutions (C_0) to the volume (V) of the uranium feed solutions used. It can be inferred from Fig. 8 that the fractional amount of uranium in the effluent (C/C_0) was negligible till 100 mL of the feed solutions, and it showed a rapid increase afterward. The sudden 'S-shaped inflection of the curve after

100 mL of the effluent reflects the presence of uranium in the effluent, otherwise known as 'Break Through.' The amount of uranium adsorbed (mg g^{-1}) up to this volume is known as break thorough capacity.

The amount of uranium adsorbed to the resin up to the break through capacity can be derived based on the area under the break through curve up to the breakthrough point, which is approximately 68.2 mg g^{-1}. Several models have been studied for different adsorption systems to investigate the dynamic column-based adsorption behavior of adsorbents. Among the different models that are studied for mathematical modeling of breakthrough behavior of fixed bed columns, the Thomas model [60, 61] is widely used, as the model assumes pseudo-second-order (PSO) reaction-based kinetics and Langmuir isotherm-based equilibrium adsorption. As the uranium adsorption to HDEHDGA resin deciphered betterboth by PSO and Langmuir adsorption isotherm models, the Thomas model is therefore expected to be valid for the present study.

A mathematical equation representing the Thomas model is shown in Eq. 11.

$$\frac{C}{C_0} = \frac{1}{1 + exp\left[\frac{k_{Th}}{Q}\left(bm - C_0 V\right)\right]} \quad (11)$$

The terms, C (μg mL^{-1}) and C_0 ((μg mL^{-1}) are the concentrations of uranium present in effluent and that of the feeds. k_{Th} is the Thomas equation constant, b is the Thomas adsorption capacity (mg g^{-1}), m is the weight of the adsorbent (g), and V is the volume of the solution (mL).

Modeling of the breakthrough capacity data, derived from the adsorption of uranium to HDEHDGA-resin, with the Thomas model, is shown in Fig. 8. The non-linear fitting parameters ($R^2 = 0.98$, $\chi^2 = 0.001$) also suggest that the experimentally derived values are in line with the prediction by the Thomas model. The breakthrough capacity deduced from the Thomas model based fitting of the breakthrough is approximately 49 mg.g^{-1}. After 150 mL, the curve shows its saturation level, known as saturation capacity (in mg g^{-1}), which is around 60 mg g^{-1} and this value is close to the adsorption values derived from the PSO and Langmuir models.

Adsorption of uranium under the influence of interfering elements

The influence of major elements present in sea water, such as Na, V, Zn, Cu, Mg, Ni, etc., could challenge the uranium adsorption was studied. Figure 9 compares uranium adsorption in the absence and in the presence of the interfering ions (Na, V, Zn, Cu, Mg, and Ni). The uranium adsorption was lowered substantially by the presence of zinc and copper and, to a smaller extent, by vanadium. It could also be seen

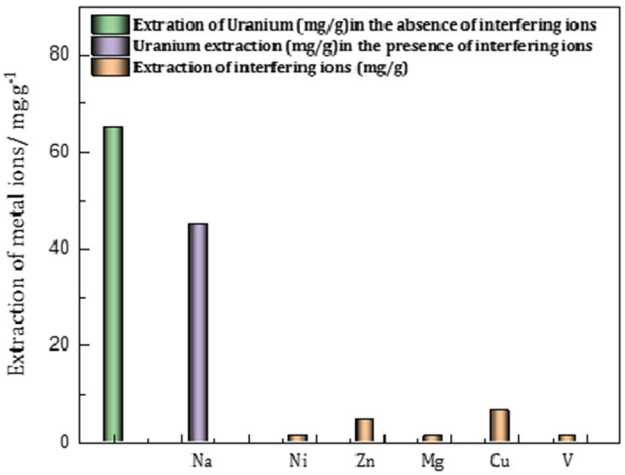

Fig. 9 Adsorption of uranium in the presence of interfering elements such as Na, Ni, Zn, Mg, Cu, and V. Adsorbent: 0.5 g of HDEHGA resin. Aqueous phase: 100 mg L-1 uranium present in sodium acetate medium at pH 6. Interfering ions (500 mg L^{-1}) each added as their respective chloride form. T = 298 K. Duration = 6 h

Table 3 Leaching studies

Sampling interval/ days	Percentage adsorption
Un-treated resin	99.0
2	98.9
5	98.1
10	97.2
20	96.1
30	94.1

Percentage of U(VI) adsorbed for different days of sampling

that sodium has not played any role in uranium adsorption. The total reduction in uranium adsorption under the presence of the above elements was only 30%. Therefore, the results of the interference study showed that HDEHDGA-coated polymeric resin offered excellent performance even in the presence of sodium and other interfering ions. Though the effect of other alkali and alkaline earth elements was not studied, the ion exchange behavior is expected to be similar to that of sodium.

Stability of coated resin and reusability

Possible leaching of diglycolamic acid from the coated resin was studied by periodic monitoring of the adsorption performance of the HDEHDGA-coated resin with uranium. Table 3 shows the adsorption tendency of the aqueous solution treated resin for uranium adsorption. It can be seen that the uranium-adsorption performance of the HDEHDGA-coated resin did not deteriorated substantially due to the

Table 4 Reusability studies

Number of recycling stages	Percentage extraction
Un-treated rersin	99.1
1	98.3
2	97.5
3	96.6
4	94.8
5	93.5

Percentage of adsorption of U(VI) as a function of number of stages of recycling

leaching of HDEHDGA to the aqueous phase. There was only less than 5% reduction of the uranium-adsorption. Since the solubility of HDEHDGA is negligible, the leaching probability of HDEHDGA is also expected to be negligible. Moreover, HDEHDGA being a bulky molecule, the leaching of HDEHDGA out of the impregnated resin matrix is expected to be minimal in aqueous environments, as reported by several authors [7, 8, 62]. Bokhove et al. [62] in their study, observed that leaching of the impregnated ligand out of the resin matrix was less when a hydrophobic ligand was employed . Maximum leaching observed for the ligand used in their system was with in 10% after several cycles of operation. Similarly, Kabay et al. [8] also have reported that the leaching of aqueous insoluble ligands will be very minimal when they are used in solvent impregnated resins. Contrast to the observations made by Bokhove et al. the leaching observed for HDEHDGA in the present system is less than 5% after 30 days of contact with aqueous phase.

For the purpose of employing the coated resin for large scale separation applications, reusability of HDEHDGA-coated resin was evaluated. It can be seen from Table 4 that the reduction in adsorption of uranium observed for the five times recycled resin was within 7%. The reduction in adsorption performance occurs after fourth recycling. However, even after five cycles of operation an adequate adsorption performance is maintained. The small amount of HDEHDGA leached out of resin matrix could be responsible for the reduction in adsorption performance. However, retaining 7% adsorption performance even after five recycling stages suggests that HDEHDGA-coated resin could be further employed for five more cycles of operations without any difficulty.

Conclusions

A cost-effective diglycolamic acid coated polymeric adsorbent was developed to separate uranium from ultra-low level uranium-bearing feed solution. The adsorbent exhibited high adsorption of uranium from aqueous solutions at pH 6. The adsorption tendency of uranium was modeled with different adsorption kinetics models, such as pseudo-first order, pseudo-second order, intra particle and film diffusion models, and different isotherm models such as Langmuir, Freundlich, Tempkin, D-R isotherms. Of all the models, the favorable kinetic model of adsorption is the pseudo-second order kinetic model and the role of film diffusion during the initial duration of adsorption cannot be ruled out. The adsorption isotherm data correlates well the Langmuir model of adsorption. Elution of uranium from the adsorbed resin phase was achieved by 0.5 M nitric acid. Modeling the adsorption behavior of uranium by diglycolamic acid resin in fixed bed column fitted well with the Thomas model. Apart from the uranium selective adsorption performance, stability to withstand in the aqueous environment with insignificant leaching of HDEHDGA and exceptional adsorption performance with recycled operations proposes that diglycolamic acid coated polyacrylic resins can be utilized for uranium separation from uranium lean aqueous solutions.

Supplementary Information The online version contains supplementary material available at https://doi.org/10.1007/s10967-023-08869-6.

Declarations

Conflict of interest The authors wish to confirm that there are no known conflicts of interest associated with this publication and there has been no significant financial support for this work that could have influenced its outcome.

References

1. Repo M, Warchoł JK, Bhatnagar A, Mudhoo A, Sillanpä M (2013) Aminopolycarboxylic acid functionalized adsorbents for heavy metals removal from water. Water Res 47:4812–4832. https://doi.org/10.1016/j.watres.2013.06.020
2. Yuan Y, Wu Y, Wang H, Tong Y, Sheng X, Sun Y, Zhou X, Zhou Q (2020) Simultaneous enrichment and determination of cadmium and mercury ions using magnetic PAMAM dendrimers as the adsorbents for magnetic solid phase extraction coupled with high performance liquid chromatography. J Hazard Mater 386:121658. https://doi.org/10.1016/j.jhazmat.2019.121658
3. Huck CW, Bonn GK (2000) Recent developments in polymer-based sorbents for solid-phase extraction. J Chromatogr A 885:51–72. https://doi.org/10.1016/j.jhazmat.2019.121658
4. Shu Q, Khayambashi A, Wang X, Wei X (2018) Studies on adsorption of rare earth elements from nitric acid solution with macroporous silica-based bis (2-ethylhexyl) phosphoric acid impregnated polymeric adsorbent. Adsorp Sci Technol 36:1049–1065. https://doi.org/10.1177/0263617417748
5. Yao L, Zhang N, Wang C, Wang C (2015) Highly selective separation and purification of anthocyanins from bilberry based on a macroporous polymeric adsorbent. J Agric Food Chem 63:3543–3550. https://doi.org/10.1021/jf506107m
6. Khayambashi A, Wang X, Wei Y (2016) Solid phase extraction of uranium (VI) from phosphoric acid medium using macroporous silica-based D2EHPA-TOPO impregnated polymeric adsorbent. Hydrometallurgy 164:90–96. https://doi.org/10.1016/j.hydromet.2016.05.013

7. Warshawsky A (1997) Solvent impregnated resins. In: Marinsky JA, Marcus Y (eds) Ion Exchange and solvent extraction: a series of advances. CRC Press, Boka Raton, pp 195–232
8. Kabay N, Cortina JL, Trochimczuk A, Streat M (2010) Solvent-impregnated resins (SIRs)–methods of preparation and their applications. React Funct Polym 70:484–496. https://doi.org/10.1016/j.reactfunctpolym.2010.01.005
9. Xiaoqi S, Yang J, Ji C, Jiutong M (2009) Solvent impregnated resin prepared using task-specific ionic liquids for rare earth separation. J Rare Earths 27:932–936. https://doi.org/10.1016/S1002-0721(08)60365-8
10. Strikovsky AG, Jeřábek K, Cortina JL, Sastre AM, Warshawsky A (1996) Solvent impregnated resin (SIR) containing dialkyldithiophosphoric acid on Amberlite XAD-2: extraction of copper and comparison to the liquid-liquid extraction. React Funct Polym 28:149–158. https://doi.org/10.1016/1381-5148(95)00060-7
11. Kahouli S (2011) Re-examining uranium supply and demand: new insights. Energy Policy 39:358–376. https://doi.org/10.1016/j.enpol.2010.10.007
12. Krymm R, Woite G (1976) Estimates of future demand for uranium and nuclear fuel cycle services. IAEA Bull 18:5
13. Parker BF, Zhang Z, Rao L, Arnold J (2018) An overview and recent progress in the chemistry of uranium extraction from seawater. Dalton Trans 47:639–644. https://doi.org/10.1039/C7DT04058J
14. Brugge D, deLemos JL, Oldmixon B (2005) Exposure pathways and health effects associated with chemical and radiological toxicity of natural uranium: a review. Rev Environ Health 20:177–194
15. Brugge D, Buchner V (2011) Health effects of uranium: new research findings. Rev Environ Health 26:231–249. https://doi.org/10.1515/REVEH.2011.032
16. Bjørklund G, Christophersen OA, Chirumbolo S, Selinus O, Aaseth J (2017) Recent aspects of uranium toxicology in medical geology. Environ Res 156:526–533. https://doi.org/10.1016/j.envres.2017.04.010
17. Ma M, Wang R, Xu L, Xu M, Liu S (2020) Emerging health risks and underlying toxicological mechanisms of uranium contamination: lessons from the past two decades. Environ Int 145:106107. https://doi.org/10.1016/j.envint.2020.106107
18. Kaufmann RF, Eadie GG, Russell CR (1976) Effects of uranium mining and milling on ground water in the Grants Mineral Belt, New Mexico. Ground Water 14:296–308. https://doi.org/10.1111/j.1745-6584.1976.tb03119.x
19. Wang J, Liu J, Li H, Song G, Chen Y, Xiao T, Qi J, Zhu L (2012) Surface water contamination by uranium mining/milling activities in northern Guangdong province. China. Clean Soil Air Water 40(2012):1357–1363. https://doi.org/10.1002/clen.201100512
20. Carvalho FP, Oliveira JM, Lopes I, Batista A (2007) Radionuclides from past uranium mining in rivers of Portugal. J Environ Radioact 98:298–314. https://doi.org/10.1016/j.jenvrad.2007.05.007
21. Durakoviæ A (1999) Medical effects of internal contamination with uranium. Croat Med J 40:49–66
22. Dehghani M, Rezaie N, Zarei M, Parseh I, Soleimani H, Keshtkar M, Zarei AA, Khaksefidi R (2022) Chemical and radiological human health risk assessment from uranium and fluoride concentrations in tap water samples collected from Shiraz, Iran; Monte-Carlo simulation and sensitivity analysis. Int J Environ Anal Chem. https://doi.org/10.1080/03067319.2022.2038145
23. Khamirchi R, Hosseini-Bandegharaei A, Alahabadi A, Sivamani S, Rahmani-Sani A, Shahryari T, Anastopoulos I, Miri M, Tran HN (2018) Adsorption property of Br-PADAP-impregnated multiwall carbon nanotubes towards uranium and its performance in the selective separation and determination of uranium in different environmental samples. Ecotoxicol Environ Saf 150:136–143. https://doi.org/10.1016/j.ecoenv.2017.12.039
24. Gan Q, Xu M, Li Q, Yang S, Yin J, Hua D (2021) Two-dimensional ion-imprinted silica for selective uranium extraction from low-level radioactive effluents. ACS Sustain Chem Eng 9:7973–7981. https://doi.org/10.1021/acssuschemeng.1c02248
25. Lee M, Ryu HJ (2016) A preliminary study for development of amidoxime-functionalized silica adsorbents for uranium (IV) extraction from seawater. IAEA INIS Technical document, INIS 48(33), Ref No. 48067267
26. Sabarudin A, Oshima M, Takayanagi T, Hakim L, Oshita K, Gao YH, Motomizu S (2007) Functionalization of chitosan with 3, 4-dihydroxybenzoic acid for the adsorption/collection of uranium in water samples and its determination by inductively coupled plasma-mass spectrometry. Anal Chim Acta 581:214–220. https://doi.org/10.1016/j.aca.2006.08.024
27. Chen B, Wang J, Kong L, Mai X, Zheng L, Zhong Q, Liang J, Chen D (2017) Adsorption of uranium from uranium mine contaminated water using phosphate rock apatite (PRA): isotherm, kinetic and characterization studies. Colloids Surf A 520:612–621. https://doi.org/10.1016/j.colsurfa.2017.01.055
28. Tang N, Liang J, Niu C, Wang H, Luo Y, Xing W, Ye S, Liang C, Guo H, Guo J, Zhang Y (2020) Amidoxime-based materials for uranium recovery and removal. J Mater Chem A 8:7588–7625. https://doi.org/10.1039/C9TA14082D
29. Zeng I, Zhang H, Sui Y, Hu N, Ding D, Wang F, Xue J, Wang Y (2017) New amidoxime-based material TMP-g-AO for uranium adsorption under seawater conditions. Ind Eng Chem Res 56:5021–5032. https://doi.org/10.1021/acs.iecr.6b05006
30. Yuan D, Chen L, Xiong X, Yuan L, Liao S, Wang Y (2016) Removal of uranium (VI) from aqueous solution by amidoxime functionalized superparamagnetic polymer microspheres prepared by a controlled radical polymerization in the presence of DPE. Chem Eng J 285:358–367. https://doi.org/10.1016/j.cej.2015.10.014
31. Ahmad M, Wang J, Yang Z, Zhang Q, Zhang B (2020) Ultrasonic-assisted preparation of amidoxime functionalized silica framework via oil-water emulsion method for selective uranium adsorption. Chem Eng J 389:124441. https://doi.org/10.1016/j.cej.2020.124441
32. Chen Y, Pan B, Zhang S, Li S, Lv L, Zhang W (2011) Immobilization of polyethylenimine nanoclusters onto a cation exchange resin through self-crosslinking for selective Cu (II) removal. J Hazard Mater 190:1037–1044. https://doi.org/10.1016/j.jhazmat.2011.04.049
33. Pranudta A, Chanthapon N, Kidkhunthod P, El-Moselhy MM, Nguyen TT, Padungthon S (2021) Selective removal of Pb from lead-acid battery wastewater using hybrid gel cation exchanger loaded with hydrated iron oxide nanoparticles: fabrication, characterization, and pilot-scale validation. J Environ Chem Eng 9:106282. https://doi.org/10.1016/j.jece.2021.106282
34. Shahadat M, Shalla AH, Raeissi AS (2012) Synthesis, characterization, and sorption behavior of a novel composite cation exchange adsorbent. Ind Eng Chem Res 51:15525–15529. https://doi.org/10.1021/ie3014555
35. Yang L, Li Y, Wang L, Zhang Y, Ma X, Ye Z (2010) Preparation and adsorption performance of a novel bipolar PS-EDTA resin in aqueous phase. J Hazard Mater 180:98–105. https://doi.org/10.1016/j.jhazmat.2010.03.111
36. Zhang C, Su J, Zhu H, Xiong J, Liu X, Li D, Chen Y, Li Y (2017) The removal of heavy metal ions from aqueous solutions by amine functionalized cellulose pretreated with microwave-H_2O_2. RSC Adv 7:34182–34191
37. Suneesh AS, Syamala KV, Venkatesan KA, Antony MP, Vasudeva Rao PR (2015) Chromatographic separation of americium (III) from europium (III) using alkyl diglycolamic acid. Sep Sci Technol 50:1213–1220

38. Ilaiyaraja P, Deb AS, Ponraju D, Ali SM, Venkatraman B (2017) Surface engineering of PAMAM-SDB chelating resin with diglycolamic acid (DGA) functional group for efficient sorption of U (VI) and Th (IV) from aqueous medium. J Hazard Mat 328:1–11
39. Naganawa H, Shimojo K, Mitamura H, Sugo Y, Noro J, Goto M (2007) A new" green" extractant of the diglycol amic acid type for lanthanides. Solvent Extr Res Dev Jpn 14:151
40. Shimojo K, Naganawa H, Noro J, Kubota F, Goto M (2007) Extraction behavior and separation of lanthanides with a diglycol amic acid derivative and a nitrogen-donor ligand. Anal Sci 23:1427
41. Shimojo K, Aoyagi N, Saito T, Okamura H, Kubota F, Goto M, Naganawa H (2014) Highly efficient extraction separation of lanthanides using a diglycolamic acid extractant. Anal Sci 30:263
42. Fatima B, Siddiqui S, Ahmed R, Chaudhry SA (2019) Preparation of functionalized CuO nanoparticles using Brassica rapa leave extract for water purification. Desalin Water Treat 164:192–205
43. Ragheb E, Shamsipur M, Jalali F, Mousavi F (2022) Modified magnetic-metal organic framework as a green and efficient adsorbent for removal of heavy metals. J Environ Chem Eng 10:107297
44. Siddiqui SI, Zohra F, Chaudhry SA (2019) Nigella sativa seed based nanohybrid composite-Fe2O3–SnO2/BC: a novel material for enhanced adsorptive removal of methylene blue from water. Environ Res 178(2019):108667
45. Bulin C, Ma Z, Guo T, Li B, Zhang Y, Zhang B, Xing R, Ge X (2021) Magnetic graphene oxide nanocomposite: one-pot preparation, adsorption performance and mechanism for aqueous Mn (II) and Zn (II). J Phys Chem Solids 156:110130
46. Boyd GE, Adamson AW, Myers LS Jr (1947) The exchange adsorption of ions from aqueous solutions by organic zeolites. II. Kinetics1. J Am Chem Soc 69:2836–2848
47. Araucz K, Aurich A, Kołodyńska D (2020) Novel multifunctional ion exchangers for metal ions removal in the presence of citric acid. Chemosphere 251:126331
48. Plazinski W (2010) Applicability of the film-diffusion model for description of the adsorption kinetics at the solid/solution interfaces. Appl Surf Sci 256:5157–5163
49. Yao C, Chen T (2017) A film-diffusion-based adsorption kinetic equation and its application. Chem Eng Res Des 119(2017):87–92
50. Ghibate R, Senhaji O, Taouil R (2021) Kinetic and thermodynamic approaches on Rhodamine B adsorption onto pomegranate peel. Case Stud Chem Environ Eng 3(2021):100078
51. GolshanTafti A, Rashidi A, Tayebi HA, Yazdanshenas ME (2018) Comparison of different kinetic models for adsorption of acid blue 62 as an environmental pollutant from aqueous solution onto mesoporous Silicate SBA-15 modified by Tannic acid. Int J Nano Dimens 9:79–88
52. Younes AA, Masoud AM, Taha MH (2018) Uranium sorption from aqueous solutions using polyacrylamide-based chelating sorbents. Sep Sci Technol 53:2573–2586
53. Yousefi SR, Ahmadi SJ, Shemirani F, Jamali MR, Salavati-Niasari M (2009) Simultaneous extraction and preconcentration of uranium and thorium in aqueous samples by new modified mesoporous silica prior to inductively coupled plasma optical emission spectrometry determination. Talanta 80:212–217
54. Youssef WM (2017) Uranium adsorption from aqueous solution using sodium bentonite activated clay. J Chem Eng Process Technol 8(2017):157–170
55. Cheira MF, Mira HI, Sakr AK, Mohamed SA (2019) Adsorption of U (VI) from acid solution on a low-cost sorbent: equilibrium, kinetic, and thermodynamic assessments. Nucl Sci Tech 30(2019):1–18
56. Zareh MM, Aldaher A, Hussein AEM, Mahfouz MG, Soliman M (2013) Uranium adsorption from a liquid waste using thermally and chemically modified bentonite. J Radioanal Nucl Chem 295(2013):1153–1159
57. Metilda P, Sanghamitra K, Gladis JM, Naidu GRK, Rao TP (2005) Amberlite XAD-4 functionalized with succinic acid for the solid phase extractive preconcentration and separation of uranium (VI). Talanta 65:192–200
58. Metilda P, Gladis JM, Rao TP (2005) Catechol functionalized aminopropyl silica gel: synthesis, characterization and preconcentrative separation of uranium (VI) from thorium (IV). Radiochim Acta 93:219–224
59. Jamali MR, Assadi Y, Shemirani F, Hosseini MRM, Kozani RR, Masteri-Farahani M, Salavati-Niasari M (2006) Synthesis of salicylaldehyde-modified mesoporous silica and its application as a new sorbent for separation, preconcentration and determination of uranium by inductively coupled plasma atomic emission spectrometry. Anal Chim Acta 579:68–73
60. Salehi E, Askari M, Darvishi Y (2020) Novel combinatorial extensions to breakthrough curve modeling of an adsorption column—depth filtration hybrid process. J Ind Eng Chem 86:232–243
61. Chittoo BS, Sutherland C (2020) Column breakthrough studies for the removal and recovery of phosphate by lime-iron sludge: modeling and optimization using artificial neural network and adaptive neuro-fuzzy inference system. Chin J Chem Eng 28:1847–1859
62. Bokhove J, Schuur B, de Haan AB (2012) Solvent design for trace removal of pyridines from aqueous streams using solvent impregnated resins. Sep Purif Technol 98:410–418